Stimulated Raman scattering of water maser lines in astrophysical plasmas

R. T. Gangadhara
Indian Institute of Astrophysics, Bangalore-560034, India

Shuji Deguchi
Nobeyama Radio Observatory, National Astronomical Observatory, Minamimaki, Minamisaku, Nagano 384-13, Japan

H. Lesch
Institut für Astronomie und Astrophysik der Universität München, Scheinerstraße 1, 81679 München, Germany

Radiative transfer equations are derived and solved for the stimulated Raman scattering of water maser lines in the astrophysical plasmas with electrons density of about $10^6 - 10^7 \, \text{cm}^{-3}$. In stimulated Raman scattering, the energy of the water maser line is transferred to the side band modes: Stokes mode and anti-Stokes mode. The Stokes mode is easily produced by backward Raman scattering while the anti-Stokes mode is created by the interacting intersecting masers in the plasma. The intensity of the Stokes mode is higher than that of the anti-Stokes mode. These side band modes are proposed as explanation for the extreme velocity features observed in the galaxy NGC 4258. The threshold value of the brightness temperature for the Raman scattering is about $10^{16} - 10^{19} \, \text{K}$, and it is satisfied in the case of NGC 4258. © *1999 American Institute of Physics.* [S1070-664X(99)02610-5]

I. INTRODUCTION

Stimulated scattering processes become important in astrophysical plasmas when the incident radiation on plasma has a very high brightness temperature ($T_b > 10^{16} \, \text{K}$).[1–4] In practice, line radiation of water masers in the galactic nuclei and continuum radiation from quasars are considered to have such a high brightness. Stimulated Raman and Compton scatterings will occur in the high and low density plasmas, respectively, depending upon whether the collective effect of electrons works or not.[5] Though a number of studies on the stimulated Raman scattering have been made, the transfer of line radiation with shifted frequency is not well understood. Fernandez and Reinnisch[6] have made an attempt to formulate the theory of stimulated Raman scattering with radiative transfer equation for specific intensities.

In this paper, we have made an attempt to study stimulated Raman scattering of the water maser line with shifted frequency. A practical application of this theory is aimed to explain the extreme high-velocity features of water maser lines at 22.235 GHz in the galactic nucleus of NGC 4258. The high-velocity features of this line appears separated by $1000 \, \text{km s}^{-1}$ from the main component of the water maser line. Though the recent Very Long Baseline Interferometry (VLBI) observations showed some evidence of this component arising from the rotating disk, all the observations (for example, the weakness of the components) are not necessarily well explained by the rotating disk model.[7] The beaming of Raman maser is discussed in Sec. II. The radiative transfer equations for stimulated Raman scattering are derived and solved in Sec. III. Further we discuss the limitation and applicability of our model to the astrophysical maser phenomenon in Sec. IV.

II. BEAMING OF RAMAN MASERS

The principal mechanism behind the beaming of astrophysical masers is the frequency change of the resonance radiation. As usual for astrophysical masers, the Raman masers are also expected to be strongly beamed. The masers are amplified in the direction with the smallest gradient in the resonance frequency where the optical depth of the resonance radiation becomes maximum. For the case of Raman masers, the change in the resonance frequency is produced by two effects: change of plasma frequency due to temperature and density variations, and Doppler effect due to the gas flow in plasma.

The frequencies of incident and scattered waves are related by

$$\omega_1 = \omega_0 - \omega_3, \tag{1}$$

where ω_0, ω_1 and ω_3 are the frequencies of incident, scattered and longitudinal waves, respectively. The frequency of the longitudinal wave is determined by the dispersion relation

$$\omega_3^2 = \omega_{pe}^2 + 3 v_t^2 k_3^2, \tag{2}$$

where $v_t^2 = k_B T / m_e$ and $\omega_{pe}^2 = 4 \pi N_e e^2 / m_e$, e and m_e are the charge and mass of electron, N_e and T are the density and temperature of electron plasma, and k_B is the Boltzmann constant.

For the case $\omega_3 \ll \omega_0$, we can approximate $k_3 = 2 \omega_0 \cos \theta_3 / c$ and $\theta_3 = (\pi - \theta_1)/2$, where θ_3 is the angle between $\mathbf{k}_0$ and $\mathbf{k}_3$, and θ_1 is the angle between $\mathbf{k}_0$ and $\mathbf{k}_1$, and c is the speed of light. Therefore, the dispersion relation can be transformed as

$$\omega_3^2 = \omega_{pe}^2 + 6(v_t^2/c^2)\omega_0^2(1 - \cos\theta_1). \tag{3}$$

In astrophysical plasmas, density and temperature of the plasma are not constant in space, and hence the resonance frequency varies along the propagation path of the waves.

In addition, the Doppler effect due to the gas flow in plasma changes the frequency, which can be expressed in the rest frame as

$$\omega_1 = [\omega_0(1 + \mathbf{v}\cdot\hat{n}_0/c) - \omega_3](1 - \mathbf{v}\cdot\hat{n}_1/c), \tag{4}$$

where $\mathbf{v}$ is the velocity of the plasma in the rest frame, and $\hat{n}_0$ and $\hat{n}_1$ are the unit vectors representing the propagation directions of incident and scattered waves, respectively.

The frequency shift along the coordinate s, which is taken in the direction of scattered wave, can be expressed as

$$\frac{d\omega_1}{ds} = \omega_0(\hat{n}_1\cdot\nabla)(\mathbf{v}\cdot\hat{n}_0/c) - \omega_{10}(\hat{n}_1\cdot\nabla)(\mathbf{v}\cdot\hat{n}_1/c)$$

$$- (\hat{n}_1\cdot\nabla)\omega_3, \tag{5}$$

where ω_{10} is the original value of frequency ω_1. The first two terms on the right-hand-side represent the frequency change due to Doppler motion of the gas, and third term is due to the density and temperature changes in plasma.

The transfer of line radiation in the moving medium has been well studied and an approximation of large velocity gradient has been developed. For example, for a spherically expanding cloud, the Doppler term (in this case $\omega_0 = \omega_1$) can be written as

$$\left(\frac{d\omega}{ds}\right)_{\text{Doppler}} = \frac{\omega_0}{c}\frac{dv}{dr}(\cos\theta_1 - 1), \tag{6}$$

where we have taken the z axis parallel to the direction of incident radiation, which is considered to be the direction of maximum optical depth ($\theta_1 = 0$). The frequency of the scattered radiation is not influenced by the Doppler motion of the matter in the case of pure-forward scattering.

The density-temperature gradient term can be written in unit of $(\omega_0/c)(dv/dr)$ as

$$\left(\frac{d\omega}{ds}\right)_{\text{D-T}} = \frac{\omega_0}{c}\frac{dv}{dr}[\cos\theta_1\{a_z + b_z(1 - \cos\theta_1)\}$$

$$+ \sin\theta_1\cos\phi_1\{a_x + b_x(1 - \cos\theta_1)\}$$

$$+ \sin\theta_1\sin\phi_1\{a_y + b_y(1 - \cos\theta_1)\}], \tag{7}$$

where vectors a and b are the nondimensional parameters, which are proportional to the density (a) and temperature (b) gradients.

III. STIMULATED RAMAN SCATTERING OF MASER

The fundamental set of equations for the study of stimulated Raman scattering in the plasma medium are

$$\frac{\partial N_e}{\partial t} + \nabla\cdot(N_e\mathbf{v}) = 0, \tag{8}$$

$$\frac{\partial\mathbf{v}}{\partial t} + \mathbf{v}\cdot\nabla\mathbf{v} = -\frac{e}{m_e}\left(\mathbf{E} + \frac{1}{c}\mathbf{v}\times\mathbf{B}\right) - \frac{3}{N_e}v_T^2\nabla N_e - \nu_c\mathbf{v}, \tag{9}$$

$$\nabla\cdot\mathbf{E} = 4\pi e(N_i - N_e), \tag{10}$$

$$\nabla\times\mathbf{E} = -\frac{1}{c}\frac{\partial\mathbf{B}}{\partial t}, \tag{11}$$

$$\nabla\times\mathbf{B} = \frac{4\pi}{c}\mathbf{j} + \frac{1}{c}\frac{\partial\mathbf{E}}{\partial t}. \tag{12}$$

Equations (8) and (9) are the electron continuity and momentum equations, respectively. Equation (10) is the Poisson equation. The last two, Eqs. (11) and (12), are Maxwell's equations. Here $\mathbf{E}$ and $\mathbf{B}$ are the electric and magnetic fields of the waves involved in the three-wave process.

Taking curl on the both sides of Eq. (11) and substituting Eq. (12) for $\nabla\times\mathbf{B}$, we get

$$\frac{\partial^2\mathbf{E}}{\partial t^2} + c^2\nabla\times(\nabla\times\mathbf{E}) + 4\pi\frac{\partial\mathbf{j}}{\partial t} = 0. \tag{13}$$

Let $N_e = N_0 + \delta N$ and $N_i = N_0$ be the electron and ion densities, respectively, where δN is the electron density perturbation induced by the ponderomotive force of the radiation field, and N_0 is the stationary background neutralizing ion density.

The current density is defined as

$$\mathbf{j} = e(N_i\mathbf{v}_i - N_e\mathbf{v}_e). \tag{14}$$

Taking the time derivative of $\mathbf{j}$ and substituting into Eq. (13), we get

$$\frac{\partial^2\mathbf{E}}{\partial t^2} + c^2\nabla\times(\nabla\times\mathbf{E}) - 4\pi e N_0\frac{\partial\mathbf{v}}{\partial t} - 4\pi e\frac{\partial(\delta N\mathbf{v})}{\partial t} = 0. \tag{15}$$

From Eq. (10), we find

$$\delta N = -\frac{1}{4\pi e}\nabla\cdot\mathbf{E}. \tag{16}$$

Using Eqs. (9) and (16), Eq. (15) can be written as

$$\frac{\partial^2\mathbf{E}}{\partial t^2} + c^2\nabla\times(\nabla\times\mathbf{E}) + \omega_{pe}^2\mathbf{E} - 3\frac{N_0}{N_e}v_T^2\nabla(\nabla\cdot\mathbf{E})$$

$$= -4\pi e N_0(\mathbf{v}\cdot\nabla\mathbf{v} + \nu_c\mathbf{v}) - \frac{\omega_{pe}^2}{c}(\mathbf{v}\times\mathbf{B}) + 4\pi e\frac{\partial(\delta N\mathbf{v})}{\partial t}. \tag{17}$$

Now, using $\mathbf{v}(\nabla\cdot\mathbf{v}) = (1/2)\nabla v^2 - \mathbf{v}\times(\nabla\times\mathbf{v})$ and $\nabla\times\mathbf{v} = e\mathbf{B}/(m_e c)$,[8] Eq. (17) can be written as

$$\frac{\partial^2\mathbf{E}}{\partial t^2} - c^2\nabla^2\mathbf{E} - \frac{3}{2}\frac{N_0}{N_e}v_T^2\nabla(\nabla\cdot\mathbf{E}) + \omega_{pe}^2\mathbf{E}$$

$$= -\frac{\partial(\mathbf{v}\nabla\cdot\mathbf{E})}{\partial t} - 2\pi e N_0\nabla v^2 - 4\pi e N_0\nu_c\mathbf{v}. \tag{18}$$

We use plane-wave approximation[9] such as

$$\mathbf{E}(\mathbf{r},t) = \frac{1}{2}\sum_{i=0-3}\{\mathbf{E}_i(\mathbf{r},t)e^{i(\omega_i t - \mathbf{k}_i\cdot\mathbf{r})}$$

$$+ \mathbf{E}_i^*(\mathbf{r},t)e^{-i(\omega_i t - \mathbf{k}_i\cdot\mathbf{r})}\} \tag{19}$$

and a similar approximation for the electron motions:

$$\mathbf{v}(\mathbf{r},t) = \frac{1}{2} \sum_{i=0-3} \{\mathbf{v}_i(\mathbf{r},t) e^{i(\omega_i t - \mathbf{k}_i \cdot \mathbf{r})}$$

$$+ \mathbf{v}_i^*(\mathbf{r},t) e^{-i(\omega_i t - \mathbf{k}_i \cdot \mathbf{r})}\}. \tag{20}$$

In Eqs. (19) and (20) the amplitudes $\mathbf{E}_i$ and $\mathbf{v}_i$ are the slowly varying functions of space and time, where $i = 0, 1, 2$ and 3 stand for incident (pump) wave $(\mathbf{k}_0, \omega_0)$, Stokes mode $(\mathbf{k}_1, \omega_1)$, anti-Stokes mode $(\mathbf{k}_2, \omega_2)$ and longitudinal plasma wave $(\mathbf{k}_3, \omega_3)$, respectively.

The stimulated Raman scattering instability excites resonantly when the following phase matching conditions are satisfied:

$$\omega_1 = \omega_0 - \omega_3, \quad \mathbf{k}_1 = \mathbf{k}_0 - \mathbf{k}_3, \tag{21a}$$

$$\omega_2 = \omega_0 + \omega_3, \quad \mathbf{k}_2 = \mathbf{k}_0 + \mathbf{k}_3. \tag{21b}$$

The growth rate of instability is given by[10,11]

$$\gamma_0 = \frac{k_3 v_0}{2} \left(\frac{\omega_{pe}}{\omega_1}\right)^{1/2}, \tag{22}$$

where $v_0 = eE_0/(m_e \omega_0)$ is the quiver velocity of the electrons in the incident radiation field.

Using the first-order approximation[9] to the electron motion we find the transfer equations for electric field amplitudes: for the incident radiation (pump)

$$\frac{\partial E_0}{\partial t} + c \frac{\partial E_0}{\partial x_0} = -c_0 E_0 - \alpha(E_1 E_3 \cos \psi_1 - E_2 E_3^* \cos \psi_2), \tag{23}$$

for the Stokes mode

$$\frac{\partial E_1}{\partial t} + c \frac{\partial E_1}{\partial x_1} = -c_1 E_1 + \alpha E_0 E_3^* \cos \psi_1, \tag{24}$$

for the anti-Stokes mode

$$\frac{\partial E_2}{\partial t} + c \frac{\partial E_2}{\partial x_2} = -c_2 E_2 - \alpha E_0 E_3^* \cos \psi_2 \tag{25}$$

and for the longitudinal wave

$$\frac{\partial E_3}{\partial t} + v_g \frac{\partial E_3}{\partial x_3} = -c_3 E_3 + \alpha_3 (E_0 E_1^* \cos \psi_1$$

$$+ E_2 E_o^* \cos \psi_2), \tag{26}$$

where $c_i = (\omega_{pe}/\omega_i)^2 \nu_c$ $(i=0,1,2,3)$ represents the free–free damping process, and the electron-ion collision frequency $\nu_c = 4\pi n_e e^4 \ln \Lambda/m_e^2 v_t^3$. The coefficients are $\alpha = k_3 e/(4m_e \omega_0)$, $\alpha_3 = \omega_{pe}^2 \alpha/(\omega_0 \omega_3)$. Here $v_g = 3v_T^2 k_3/\omega_3$ is the group velocity of longitudinal wave and ψ_i $(i=1$ or 2) is the angle between $\mathbf{E}_0$ and $\mathbf{E}_1$ or $\mathbf{E}_2$. The coordinates x_i $(i=0,1,2,3)$ represent the direction of propagation of each wave.

Only the frequency downshifted component (Stokes mode) is excited, and the upshifted component (anti-Stokes mode) is not amplified at the general scattering angles even if it is resonant.[10,12] It should be noted that the second terms on the right-hand-side of Eqs. (24) and (25) are plus and minus. This means that only the downshifted waves grow, but the

upshifted waves never grow. However, the resonance can occur for either of the upshifted or downshifted components in general, but both the components appear only in the case of pure-forward scattering.[17]

For the longitudinal wave, Landau damping is more efficient than the binary collisional damping. The Landau damping rate of the plasma wave is given by

$$\Gamma = \left(\frac{\pi}{8}\right)^{1/2} \frac{(\omega_{pe}\omega_3)^2}{(|k_3| v_T)^3} \exp[-\omega_3^2/(2|k_3| v_T)^2]. \tag{27}$$

In the steady state, Eqs. (23), (24) and (26) reduces to

$$\frac{\partial E_0}{\partial x_0} = -\frac{c_0}{c} E_0 - \frac{\alpha}{c} E_1 E_3, \tag{28}$$

$$\frac{\partial E_1}{\partial x_1} = -\frac{c_1}{c} E_0 + \frac{\alpha}{c} E_0 E_3^*, \tag{29}$$

$$E_3 = \frac{\alpha_3}{\Gamma + c_3} E_0 E_1^*, \tag{30}$$

where we have assumed incident wave and scattered wave are polarized in the same direction $(\psi_1 = 0)$. Eliminating E_3 between the Eqs. (28) and (30), we find

$$\frac{\partial E_0}{\partial x_0} = -\frac{c_0}{c} E_0 - \frac{\alpha \alpha_3}{c(\Gamma + c_3)} |E_1|^2 E_0. \tag{31}$$

The complex conjugate of Eq. (31) is given by

$$\frac{\partial E_0^*}{\partial x_0} = -\frac{c_0}{c} E_0^* - \frac{\alpha \alpha_3}{c(\Gamma + c_3)} |E_1|^2 E_0^*. \tag{32}$$

Multiplying Eq. (31) by E_0^* and Eq. (32) by E_0, and adding, we get

$$\frac{\partial I_0}{\partial x_0} = -\frac{2c_0}{c} I_0 - \frac{2\alpha \alpha_3}{c(\Gamma + c_3)} I_1 I_0. \tag{33a}$$

Similarly from Eq. (29), we find

$$\frac{\partial I_1}{\partial x_1} = -\frac{2c_1}{c} I_1 + \frac{2\alpha \alpha_3}{c(\Gamma + c_3)} I_0 I_1, \tag{33b}$$

where $I_0 = |E_0|^2$ and $I_1 = |E_1|^2$ are the intensities of the incident and scattered waves. In Eq. (33) the first term on the right-hand-side represent the free–free collisional damping. While the second term in Eq. (33a) represents stimulated absorption of the incident radiation and in Eq. (33b) it represents the stimulated emission of the scattered radiation.

A. Solution of Eq. (33)

When the amplitudes of I_0 and I_1 are not too large, we solve Eq. (33) numerically. But when I_0 and I_1 are too large we can ignore the collisional damping terms and find the analytical solutions.

The direction of propagation of the incident and the scattered waves in the thick and the thin plasma media are shown in Fig. 1. Let θ be the angle between the coordinates x_0 and x_1, then we have $x_0 = x_1 \cos \theta$, and Eq. (33) becomes

$$\frac{dI_0}{ds} = -\cos(\theta) \left[I_0 + \frac{B_0}{A_0} I_1 I_0 \right], \tag{34a}$$

Phys. Plasmas, Vol. 6, No. 10, October 1999

Stimulated Raman scattering of water maser lines in . . .   4091
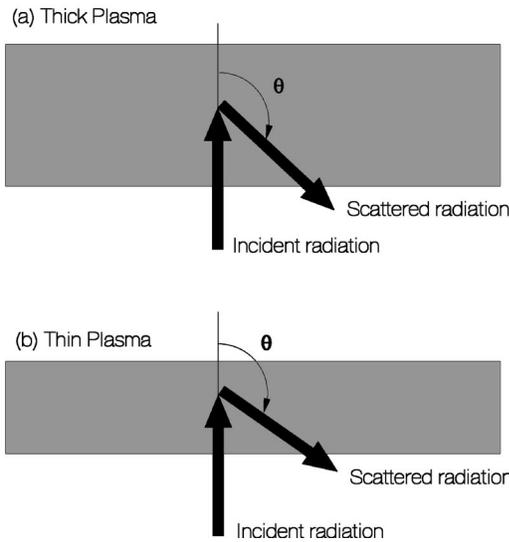
FIG. 1. The scattering geometry of the incident maser radiation in the case of thick plasma (a) and thin plasma (b) media.

FIG. 2. The incident wave intensity I_0/I_c and scattered wave intensity I_1/I_c vs s in the case thick plasma medium at different scattering angles $\theta = 120°, 140°, 160°$ and $180°$. I_c is a normalization constant and the parameter $s = (2\nu_c\omega_{pe}/c\omega_0)x_1$.

$$\frac{dI_1}{ds} = -\frac{A_1}{A_0}I_1 + \frac{B_1}{A_0}I_1 I_0, \tag{34b}$$

where $ds = A_0\,dx_1$, $A_0 = 2c_0/c$, $B_0 = \alpha\alpha_3/\{c(\Gamma + c_3)\}$, $A_1 = 2c_1/c$, and $B_1 = B_0$.

Defining $W_0 = \log(I_0/I_c)$ and $W_1 = \log(I_1/I_c)$, where I_c is a normalization constant, we write Eq. (34) as

$$\frac{dW_0}{ds} = -\cos(\theta)\left[1 + \frac{B_0}{A_0}I_c\exp(W_1)\right], \tag{35a}$$

$$\frac{dW_1}{ds} = -\frac{A_1}{A_0} + \frac{B_1}{A_0}I_c\exp(W_0). \tag{35b}$$

We numerically solve Eq. (35) using the plasma density $N_0 = 3\times10^6\,\text{cm}^{-3}$, the electron temperature $T = 4200\,\text{K}$, frequency of the incident radiation $\nu_0 = 22.235\,\text{GHz}$ and $I_c = A_0/B_0$.

The incident and the scattered wave intensities as functions of s, at different values of the scattering angle $\theta = 120°, 140°, 160°$ and $180°$ in a thick plasma medium, are plotted in Fig. 2. At $s = 0$, we started with initial conditions $I_0/I_c = 1$ and $I_1/I_c = 10^{-30}$. As s increases scattered wave intensity grows much faster than incident wave intensity, indicating transfer of energy from the incident wave to the scattered wave. At large s, say 3.6, and $\theta = 180°$, intensity of the incident wave becomes very large, consequently, the scattered mode also becomes much stronger. The range of s, over which the incident and the scattered waves interact, increases with decreasing θ. Similarly, Fig. 3 shows the incident wave and the scattered wave intensities as functions of s, at different values of the scattering angle $\theta = 120°, 140°, 160°$ and $180°$ in the case of thin plasma medium. Again at $s = 0$, we started with initial conditions $I_0/I_c = 10^3$ and $I_1/I_c = 10^{-30}$. At large s, say 1, and $\theta = 180°$, intensity of the incident wave becomes very large, consequently, scattered mode also becomes much stronger.

When the stimulated absorption of I_0 and emission of I_1 are very large compared to free–free absorption rates we can ignore the collisional damping terms in Eq. (33), therefore, we have

$$\frac{dI_0}{ds} = -\cos(\theta)\frac{B_0}{A_0}I_1 I_0, \tag{36a}$$

$$\frac{dI_1}{ds} = \frac{B_1}{A_0}I_0 I_1. \tag{36b}$$

Solutions of Eq. (36) can easily be obtained using the following convenient transformations:[13]

$$U_0 = \frac{B_1}{A_0}I_0, \quad U_1 = \cos(\theta)\frac{B_0}{A_0}I_1. \tag{37}$$

Now, Eq. (36) becomes
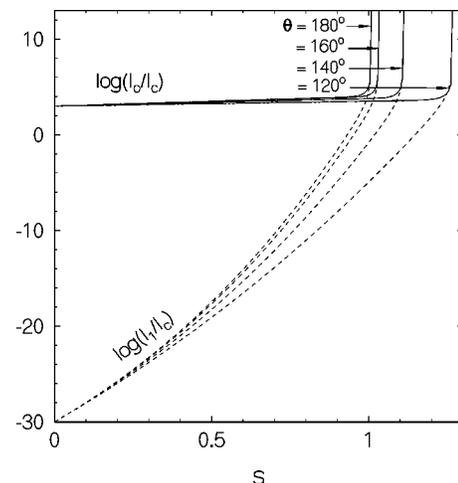
FIG. 3. The incident wave intensity I_0/I_c and scattered wave intensity I_1/I_c vs s in the case thin plasma medium at different scattering angles $\theta = 120°, 140°, 160°$ and $180°$. I_c is a normalization constant and the parameter $s = (2\nu_c\omega_{pe}/c\omega_0)x_1$.
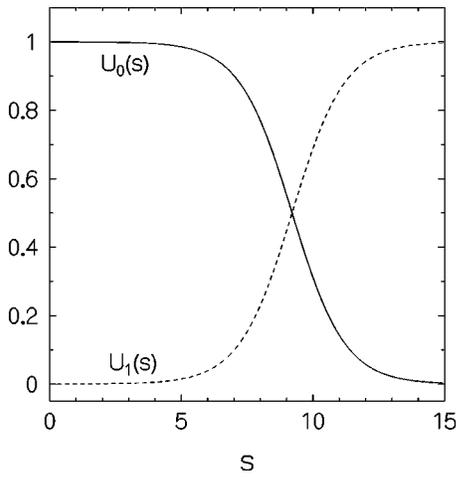
FIG. 4. Energy transfer between the coupled modes ($U_0(s)$ corresponding to the pump wave) and the parameter $s = (2\nu_c \omega_{pe}/c\omega_0)x_1$.

$$\frac{dU_0}{ds} = -U_1 U_0, \tag{38a}$$

$$\frac{dU_1}{ds} = U_0 U_1. \tag{38b}$$

In the case of forward Raman scattering, we can define a constant of motion

$$U_0(s) + U_1(s) = m = U_0(0) + U_1(0), \tag{39}$$

the solutions of Eq. (38) can then be written as

$$U_0(s) = \frac{m U_0(0)}{U_0(0) + U_1(0)\exp(ms)}, \tag{40a}$$

$$U_1(s) = \frac{m U_1(0)}{U_1(0) + U_0(0)\exp(-ms)}. \tag{40b}$$

The s dependence of the solutions is depicted in Fig. 4. We notice that the energy from the pump will get monotonically transferred to the scattered mode.

B. Production of the anti-Stokes component by intersecting masers

It is clear from the previous section that the downshifted component can be easily created in astrophysical conditions. However, the upshifted component can only be produced in the forward Raman scattering, which requires brightness temperature of the order of 10^{25} K, and it is impossible to reach in astrophysical masers.

We propose a special mechanism by invoking an inhomogeneity in the plasma to explain the upshifted features seen in the spectrum of NGC 4258. The possibility of enhancing the forward scattering by the backward scattering in the plasma, which has parabolic density profile[14,15] or by coupling Raman scattering with Brillouin scattering in the backward scattering[16] has been known from the experiments on laser-plasma interactions in the laboratory plasma.

Suppose two maser beams are intersecting in the plasma. If the maser beams are intersecting in such a way that they produce the same longitudinal wave at the same direction,

then the energy transfer can take place between the two maser beams. In this process, the longitudinal wave produced by the backward scattering of the incident radiation is exactly frequency matched with the upshifted scattered wave produced by the other incident radiation. The threshold condition for the backward Raman scattering is

$$W_{thr} = \frac{\alpha\alpha_3}{c_1 c_3}|E_0|^2 \cos^2\psi_1 > 1. \tag{41}$$

The frequencies of the two intersecting maser beams need not be exactly the same. The threshold condition implies that the intersecting angle of two masers has an allowance of about $\pm 10°$ because $\mathbf{k}_1$ and $\mathbf{k}_3$ have a beam angle of this order of magnitude.

In this case, the transfer equations become very similar to Eqs. (24)–(26) as

$$\frac{\partial E_1}{\partial t} + c\frac{\partial E_1}{\partial x_1} = -c_1 E_1 + \alpha E_0 E_3^* \cos\psi_1, \tag{42}$$

$$\frac{\partial E_2'}{\partial t} + c\frac{\partial E_2'}{\partial x_2'} = -c_2 E_2' - \alpha E_0' E_3^* \cos\psi_2', \tag{43}$$

and

$$\frac{\partial E_3}{\partial t} + v_g\frac{\partial E_3}{\partial x_3} = -c_3 E_3 + \alpha_3(E_0 E_1^* \cos\psi_1$$
$$+ E_2' E_0'^* \cos\psi_2'), \tag{44}$$

where the primed quantities are for the second maser beam, and $\mathbf{k}_2' - \mathbf{k}_0' = \mathbf{k}_3$. In this process, the perfect phase matching is achieved for both the upshifted and downshifted components, and we can repeat the analysis similar to the former treatment (Sec. III). The growth rate is obtained as

$$\gamma = \frac{\alpha\alpha_3}{c_3}\left(\frac{|E_0|^2}{c_1}\cos^2\psi_1 - \frac{|E_0'|^2}{c_1}\cos^2\psi_2'\right)c_0. \tag{45}$$

For $\psi_1 = \psi_2' = 0$, the threshold condition is

$$(|E_0|^2 - |E_0'|^2)\frac{\alpha\alpha_3}{c_3}c_0 > 1. \tag{46}$$

Therefore in order to excite the upshifted component the intensity of the first incident maser must be greater than the intensity of the second maser.

IV. RESTRICTIONS OF THE THEORY

We have not included the incoherency effect due to the incident maser radiation. The bandwidth and maser beam solid angle determine the coherence scale length. If we take the maser beam solid angle to be 10^{-4} and the bandwidth of 1 km/s, we can evaluate the coherency length approximately as $L_c = \lambda(\Delta\Omega)^{-1}$ or $L_c = \lambda c/\Delta v_0 \approx 10^4 - 10^5\lambda$, where λ is the wavelength of the maser radiation. The Landau damping time of the longitudinal plasma wave is one order of magnitude higher than the coherence time scale ($\sim 10^{-5}$ s) of the incident radiation. Hence the monochromatic approximation used in the present analysis seems to be a good approximation. The effect of incoherence on the growth rate of stimulated Raman scattering is discussed in Ref. 11. The second

order Raman scattering of side band modes and the intensity level of the incident radiation are the main factors in limiting (saturating) the amplitude of the side band modes.

V. CONCLUSION

The threshold condition for backward stimulated Raman scattering is satisfied in the case of NGC 4258.[9] If the compact HII regions are located near the center of maser cloud, maser beam intersections can occur in it and the upshifted component can also be produced when the maser beams interact by coupling with a longitudinal plasma. Figures 2 and 3 indicate the length scales for the amplification of wave amplitudes in thick and thin plasma media, respectively. The inhomogeneity in the plasma and bandwidth in the incident radiation can increase the amplification length by one order of magnitude.

The growth rate of stimulated Raman scattering is very large in the case of backward scattering than that in forward scattering. This leads to the complexity in explaining the spectrum and time variability of extreme features.

The red and blue shifted features could be independent and produced by two separate masers. A crucial test for the stimulated Raman maser model is finding the triplet with an equal separation and not finding a coherent time variation for the upshifted and downshifted components.

ACKNOWLEDGMENTS

[1] V. Krishan, Astrophys. Lett. **23**, 133 (1983).

[2] V. Krishan, Curr. Sci. **64**, 301 (1993).

[3] V. Krishan and P. J. Wiita, Mon. Not. R. Astron. Soc. **246**, 597 (1990).

[4] V. Krishan and P. J. Wiita, Astrophys. J. **423**, 172 (1994).

[5] R. T. Gangadhara and V. Krishan, Mon. Not. R. Astron. Soc. **256**, 111 (1992).

[6] C. Fernandez and G. Reinnisch, Astron. Astrophys. **67**, 163 (1978).

[7] M. Miyoshi, J. Moran, J. Herrnstein, L. Greenhill, N. Nakai, P. Diamond, and M. Inoue, Nature (London) **373**, 127 (1995).

[8] C. J. McKinstrie, A. Simon, and E. A. Williams, Phys. Fluids **27**, 2738 (1984).

[9] S. Deguchi, Astrophys. J. **420**, 551 (1994).

[10] R. T. Gangadhara and V. Krishan, Astrophys. J. **415**, 505 (1993).

[11] K. L. Kruer, *The Laser Plasma Interactions* (Addison-Wesley, Redwood City, CA, 1988), p. 90.

[12] R. T. Gangadhara and V. Krishan, Astrophys. J. **440**, 116 (1995).

[13] D. Anderson, Phys. Scr. **13**, 117 (1976).

[14] P. Koch and E. A. Williams, Phys. Fluids **27**, 2346 (1984).

[15] R. E. Turner, K. Estarbrook, R. P. Drake, E. A. Williams, H. N. Kornblum, W. L. Kruer, and E. M. Campbell, Phys. Rev. Lett. **57**, 1725 (1986).

[16] C. Labaune, H. A. Baldis, S. D. Baton, D. Pesme, and T. Jalinaud, Phys. Rev. Lett. **69**, 285 (1992).

[17] C. Labaune, H. A. Baldis, B. Chen, W. Rozmus, S. Depierreux, E. Schifano, B. S. Bauer, and A. Michard, Phys. Plasmas **6**, 2048 (1999).